$Na_4P_2O_7$, 13.2; $K_4P_2O_7$, 45.0; and H_2O, 41.8 weight %. Data used in the development of this diagram and for the other three isotherms are given in tabular form.

The $K_4P_2O_7$-rich area shows a high solubility and an equilibrium solid phase which accepts $Na_4P_2O_7$ as an isomorphous adjunct. The convergence of experimentally determined tie lines is interpreted as a reflection of the curvature of the solubility line. These lines terminate in a hydrated solid solution rather than a crystalline double salt composition. The composition of the solid solution may be expressed as $(aK_4P_2O_7 \cdot bNa_4P_2O_7) \cdot 3(a + b)H_2O$, where $0 < a < 0.77$ and $a + b = 1.00$.

A series of x-ray diffraction patterns made from solids in this area was compared with the pattern for $K_4P_2O_7 \cdot 3H_2O$, the equilibrium solid phase from the $K_4P_2O_7$-H_2O system at 25° C., and the pattern for $Na_4P_2O_7 \cdot 10H_2O$, the equilibrium solid phase from the $Na_4P_2O_7$-H_2O system at 25° C. No new or different crystalline phase was indicated, although orientation effects caused some variation in line intensities.

The section of decreasing $K_4P_2O_7$ concentration moving from the invariant composition has an equilibrium crystalline solid phase of $Na_4P_2O_7 \cdot 10H_2O$, the only known hydrate of $Na_4P_2O_7$.

In figure 1, both solubility lines extrapolate from the invariant point into the two-phase areas so that the thermodynamic requirements for an isothermal junction are satisfied (*5*).

The shape of the solubility line in the $Na_4P_2O_7 \cdot 10H_2O$ area indicates that $K_4P_2O_7$ has a salting in effect when added to excess $Na_4P_2O_7$ in water.

The 50° C. isotherm shown in Figure 2 has the same form as the 25° C. isotherm, with $Na_4P_2O_7 \cdot 10H_2O$ and a hydrated solid solution as equilibrium solid phases. A hydrate transition was observed in the equilibrium solid phase between initial compositions containing 55.5% $K_4P_2O_7$ and 52.2% $K_4P_2O_7$ at a constant $Na_4P_2O_7$ concentration. This change in the solid phase is best interpreted as a transition from a trihydrate to a hexahydrate. This conclusion was based on composition analysis of wet-residue which was filtered at 50° C. to remove all but traces of the saturated liquor. No break was observed in the solubility line to correspond with this change in the solid phase.

The solubility lines for 10° and 85° are shown in Figure 3. The degree of hydration of the solid solution was not determined for these two temperatures.

ACKNOWLEDGMENT

The discussions and criticisms of E.J. Griffith throughout the course of this work are gratefully acknowledged.

LITERATURE CITED

(1) Griffith, E.J., Callis, C.F., *J. Am. Chem. Soc.* 81, 833 (1959).
(2) Morey, G.W., others, *Ibid.*, 77, 5003 (1955).
(3) Schreinemakers, F.H.H., *Z. phys. Chem.* 11, 75 (1893).
(4) Van Wazer, J.R., "Phosphorus and Its Compounds," Vol. 1, p. 625, Interscience, New York, 1958.
(5) Williamson, E.D., Morey, G.W., *J. Am. Chem. Soc.* **40**, 49 (1918).

Received for review July 5, 1960. Accepted January 9, 1961.

Solubilities of Some Heteropoly Salts in Aqueous Solutions

KARLO F. SCHULZ, EGON MATIJEVIĆ, and MILTON KERKER, Clarkson College of Technology, Potsdam, N.Y.

IN A STUDY of some heteropoly compounds, it became necessary to determine the composition of several salts of these compounds as well as their solubilities. The electromotive force (e.m.f.) data of cells consisting of tungstophosphoric acids and mercury-mercurous tungstophosphate electrodes (*3*) could not be interpreted because of lack of knowledge of the composition of the solid phase of the mercurous tungstophosphate and of solubility data. These compounds were obtained by precipitation of 12-tungstophosphoric acid with mercurous nitrate by O.W. Gibbs as early as the second half of the last century and by H. Copaux at the beginning of this century (*10*). However, no quantitative data on composition or solubility were reported. In fact, the only quantitative data located were those of Rakovskii and Nikitina on tungstophosphoric acid, tungstomolybdic acid, and some of their sodium salts (*12*). Again, in studying the coagulation effects of 12-molybdoceric(IV) acid upon positive silver halide sols, the solubility of silver 12-molybdocerate(IV) had to be known (*9*). This slightly soluble salt was originally prepared by Barbieri (*1*), but its solubility had not been determined.

Vouk, Kratohvil, and Tezak (*16*) have shown that if the solid phase is known, the complex ionic species in equilibrium with solid silver halides can be determined by analysis of the general solubility curves (*7, 13*). Such curves are constructed from solubility data obtained in an excess of either component as well as in the presence of equivalent concentrations of each. In this work their method has been extended to the determination of the solid species.

The general solubility curves of silver 12-molybdocerate(IV), mercurous 12-tungstophosphate, and mercurous 9-tungstophosphate were determined, and from these solubility data conclusions as to the composition of the solid phase as well as the species of soluble complex ions could be drawn. In addition, the effect of pH upon solubility was studied for the two mercurous tungstophosphates.

EXPERIMENTAL

Method. Solubility was determined by a procedure described previously (*13, 16*). The sparingly soluble heteropoly salt was precipitated in the nascent state by mixing solutions of the two precipitating components—*viz.*, the heteropoly acid and a metal salt. The precipitation limit was determined by mixing 5 ml. of a solution of one precipitating component (usually the heteropoly acid) of constant concentration with 5 ml. of solutions containing the other component in various (gradually decreasing) concentrations. The concentrations of the variable component were always higher than the concentration of the constant component. All concentrations were calculated for the final volume of 10 ml. and expressed as molarities. Nitric acid was added to one of the components when it was required to adjust the pH. The limiting precipitation concentration was determined by measuring the turbidity of mixed solutions. If turbidity is plotted against concentration of the variable component, a very sharp increase in turbidity is observed in the range where the precipitate is formed. The limiting precipitation concentration can be obtained when the steep part of the turbidity-concentration curve is extrapolated to zero turbidity.

Limiting precipitation concentrations were obtained for a large number of concentrations of the constant component, always choosing an appropriate concentration gradient of the excess component. Sometimes the experiment was reversed and the metal salt was kept constant, whereas the concentration of the heteropoly acid was gradually changed. This provided a check on the validity of the technique.

The turbidity was obtained from light-scattering intensity measurements using a light scattering microphotometer (Aminco). The angle of observation was 45° and the wave length 546 mμ. All solutions were kept in stoppered test tubes at 25° ± 0.05° C. in a constant temperature bath. Turbidity changes were followed over a period of time varying from a few days to 2 weeks. The precipitation process was considered completed when no further precipitate was formed in any test tube for at least 2 days. At very low concentrations of reacting components, turbidity measurements became precarious because the solid phase formed a small number of macroscopic crystals instead of a colloidal suspension. These tended either to settle out or to float and in such cases observations were made visually. When visual observation was used, the concentration of the component in excess was chosen as the mean of the concentration at which no precipitate was observed and that at which the first trace of precipitate appeared. The average deviation of all duplicate determinations was less than 10%.

Precipitation determinations for the tungstophosphoric acids were made at constant pH's. These were adjusted by adding a suitable amount of nitric acid to the precipitating systems and measuring with a Beckman Model G pH meter with glass electrode.

Materials. 12-Tungstophosphoric acid, $H_3PW_{12}O_{40}(s)$ or $H_7PW_{12}O_{42}$ (Baker analyzed reagent), was carefully purified. 9-Tungstophosphoric acid, $H_6P_2W_{18}O_{62}$, and 12-molybdoceric(IV) acid, $H_8CeMo_{12}O_{42}$, were synthesized following procedures for preparation and purification (*8, 9*).

Mercurous nitrate, $HgNO_3 \cdot H_2O$ (Fisher certified reagent), solutions were analyzed for mercury content by utilizing the standard electrolytic procedure (*15*). All other chemicals used were commercial chemicals of highest purity grades. Solutions were prepared with doubly distilled water, the second distillation being carried out in an all-borosilicate glass still. Glassware was cleaned with chromic acid solution and was well steamed before use.

RESULTS AND DISCUSSION

Silver 12-Molybdocerate(IV). The logarithm of the silver ion concentration (expressed in molarities) is plotted against the logarithm of the molar concentration of the 12-molybdoceric(IV) acid (Figure 1). When solutions of precipitating components are mixed in concentration ratios below and to the left of the curve, the precipitate does not appear, whereas it is formed when solutions in concentrations above and to the right of the solubility line are mixed together. This curve is referred to as the general solubility curve.

The curve shows four very distinct ranges which are practically linear and have slopes *b* equal to +2, −8, −3, and −0.5, respectively. The narrow range *A* on both sides of the equivalent line gives the solubility limit for the solid phase $Ag_8CeMo_{12}O_{42}$ against its true ionic solubility. The composition of this solid phase had been determined analytically (*1*). The stoichiometric solubility product, K_{sp}, for points in this range equals 7.8×10^{-36}. This value is slightly lower than that reported in the fourth article of this series (*9*), where one extra point (for 2×10^{-4} *M* Ag^+) was used in averaging the solubility product. After completing the solubility curve, it became obvious that this point fits better into range *C*. In calculating K_{sp}, the stoichiometric concentration of $H_8CeMo_{12}O_{42}$ was used because for this low concentration range (10^{-5} to $10^{-7}M$) the acid is practically completely ionized (*9*).

Abrupt changes in slopes of the general solubility curve usually indicate the existence of soluble ionic complexes which are responsible for such changes. Composition of the predominant complex species and their stability constants can be evaluated by utilizing a graphical analysis of solubility curves if these are plotted as shown in Figure 1 (*6*). For this case the analysis can be performed as follows.

If solid $Ag_8CeMo_{12}O_{42}$ (Ag_8X, $X^{-8} = CeMo_{12}O_{42}^{-8}$) forms complex ions upon being dissolved in excess of Ag^+, the following equilibrium must exist, assuming the ions to be mononuclear with respect to the heteropoly anion.

$$Ag_8X(s) \rightleftarrows Ag_nX^{n-8} + (8-n)Ag^+ \qquad (1)$$

The equilibrium constant is

$$K'_n = \frac{[Ag_nX^{n-8}][Ag^+]^{8-n}}{[Ag_8X(s)]} \qquad (2)$$

or since the activity of the solid phase is constant

$$K_n = [Ag_nX^{n-8}][Ag^+]^{8-n} \qquad (3)$$

The stability constant, κ_n, for the complex ion Ag_nX^{n-8} is

$$n\,Ag^+ + X^{8-} \rightleftarrows Ag_nX^{n-8} \qquad (4)$$

and

$$\kappa_n = \frac{[Ag_nX^{n-8}]}{[Ag^+]^n[X^{8-}]} \qquad (5)$$

Combination of Equations 3 and 5 gives

$$K_n/\kappa_n = [Ag^+]^8[X^{8-}] = K_{sp} \qquad (6)$$

The straight lines in Figure 1 can obviously be represented

$$\log [H_8X]_t = \log a + b \log [Ag^+] \qquad (7)$$

where $[H_8X]_t$ is the stoichiometric concentration of the acid and *b* is given by the slopes indicated on the diagram. If Equation 3 is written in logarithmic form, and if only mononuclear complexes are present

$$\log [H_8X]_t = \log K_n - (8-n) \log [Ag^+] \qquad (8)$$

since for mononuclear species and strong complex formation

$$[Ag_nX^{n-8}] \cong [H_8X]_t \qquad (9)$$

It follows, therefore, that

$$b = n - 8 \qquad (10)$$

$$a = K_n \qquad (11)$$

In range *A*, it is rather difficult to assign the slope precisely because of the large value of the slope and the small extent of this range. However, the slope is approximately 8, in which case it appears that the salt is fully ionized into silver ions and molybdocerate(IV) ions. In range *C*, however, *n* equals 5, and therefore the predominant complex species in solution is $Ag_5CeMo_{12}O_{42}^{-3}$. In range *D*, a mixture of species must exist, since slope $b = -0.5$ gives $n = 7.5$. The simplest way to interpret this is to assume an equimolar mixture of soluble species $Ag_7CeMo_{12}O_{42}^{-1}$ and $Ag_8CeMo_{12}O_{42}$. It is difficult to decide whether this assumption is correct, because a mixture of other species could by coincidence also give a value for $n = 7.5$.

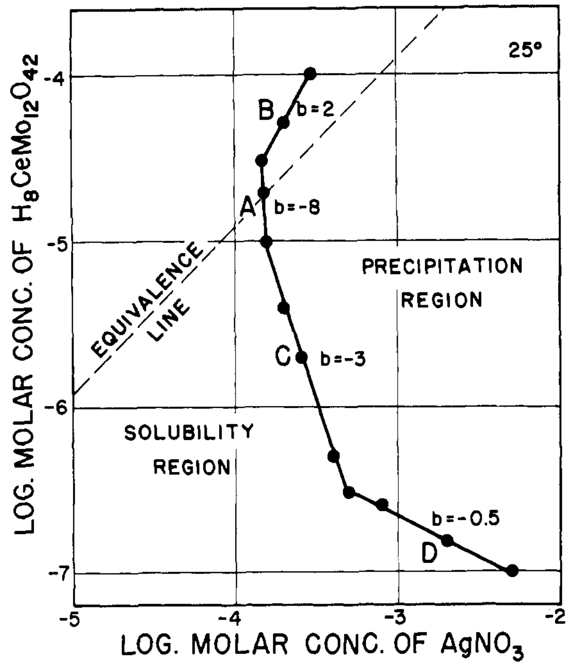

Figure 1. General solubility curve for silver salt of 12-molybdoceric(IV) acid

From Equation 6 the stability constant for the relevant complex species can be calculated from the solubility product, K_{sp}, and the equilibrium constant K_n. K_n can be obtained from Equations 3 and 9. The calculated stability constant for the species $Ag_5CeMo_{12}O_{42}^{-3}$ is 7.0 × 10^{18}, indicating a very strong complex.

Finally, for range *B*, an analogous analysis for complex ions in excess of the heteropoly anion can be performed. Since, in this case, polynuclear complex species may be expected, the relationship between the slope, *b*, and number of ligands, *n*, will be different from that given in Equation 10. Such an analysis was made, but the insufficient data in this range did not allow unambiguous conclusions. Still another difficulty arises in this range of greater concentration of the heteropoly ions—viz., the ionic strength influence of such highly charged ions upon these equilibria.

Mercurous 12-Tungstophosphate. General solubility curves for the mercurous salt of the 12-tungstophosphoric acid for three different pH values are given in Figure 2. At the pH's investigated, the curves show two distinctly different ranges denoted as *A* and *B*. Range *A* has the same slope for all three curves—viz., $b = -2$. The composition of the solid phase of the mercurous tungstophosphates could not be determined by direct analysis. Repeated efforts always yielded inordinately large amounts of mercury, apparently due to occlusion of $HgNO_3$. However, the following analysis of data in Figure 2 leads to $Hg_2HPW_{12}O_{40}$ for the composition of the solid phase in range *A*.

On the basis of x-ray analysis, it appears that in crystalline 12-tungstophosphates the anions have a −3 charge (*2, 5, 11, 14*). In solution, 12-tungstophosphoric acid is heptabasic, giving in dilute solutions the corresponding −7 charged anion (*9*). Accordingly, the solid will be designated as $H_3PW_{12}O_{40}(s)$ and the species in solution as $H_7PW_{12}O_{42}$, $H_6PW_{12}O_{42}^{-1}, \ldots, PW_{12}O_{42}^{-7}$.

In accordance with this, the solid will be treated as consisting of completely dissociated tribasic heteropoly anion, $PW_{12}O_{40}^{-3}$, but in solution the hydrolyzed ions such as $PW_{12}O_{42}^{-7}$ or corresponding protonated species will be considered. Also, only one solid species that is monomeric with respect to the heteropoly anion will be assumed. Accordingly, the solution equilibrium can be represented by

$$Hg_nH_{3-n}PW_{12}O_{40}(s) + 2H_2O \rightleftarrows n\,Hg^+ + H_{7-n}PW_{12}O_{42}^{-n} \quad (12)$$

and

$$[Hg^+]^n\,[H_{7-n}PW_{12}O_{42}^{-n}] = K_{sp} \quad (13)$$

The concentrations of the various anionic species are

$$[H_{7-n}PW_{12}O_{42}^{-n}] = \prod_{i=1}^{n} K_i[H_7PW_{12}O_{42}]/[H^+]^n \quad (14)$$

where K_i refers to successive ionization constants for the acid. At constant pH, $[H_7PW_{12}O_{42}]$is directly proportional to the stoichiometric acid concentration, $[H_7PW_{12}O_{42}]_t$

$$[H_7PW_{12}O_{42}]_t = \{1 + \sum_{j=1}^{7} (\prod_{i=1}^{j} K_i/[H^+]^j)\}[H_7PW_{12}O_{42}] \quad (15)$$

$$[H_7PW_{12}O_{42}]_t = k'\,[H_7PW_{12}O_{42}] \quad (15a)$$

so that

$$[H_{7-n}PW_{12}O_{42}^{-n}] = \frac{\prod_{i=1}^{n} K_i[H_7PW_{12}O_{42}]_t}{k'[H^-]^n} = k[H_7PW_{12}O_{42}]_t \quad (16)$$

and

$$[Hg^+]^n\,[H_7PW_{12}O_{42}]_t = K_{sp}/k_n = [K_{sp}] \quad (17)$$

where $[K_{sp}]$ is an apparent solubility product constant. The values of $[K_{sp}]$ were 9.0 × 10^{-10} at pH = 1.10, 1.2 × 10^{-11} at pH = 1.58, and 9.6 × 10^{-13} at pH = 2.02.

The value of *n* can be obtained from the slope of a plot of $\log[Hg^+]$ against $\log[H_7PW_{12}O_{42}]_t$ (Figure 2), from which it is apparent that in region *A* for each of the pH's investigated, the solid phase is $Hg_2HPW_{12}O_{40}$. Formation of acid salts of 12-tungstophosphoric acid is a common effect, and a number of other acid salts have been characterized and described (*4, 10, 17*).

Figure 2 shows that the solubility of $Hg_2HPW_{12}O_{40}(s)$ is influenced strongly by the acidity of the medium. This is probably due to the combined influence of the added acid (HNO_3) upon the ionization equilibria and the activities of the various species. Solubility increases with decreasing pH as would be expected, if the heteropoly acid were primarily in the form of doubly and lower charged species. The concentration of the $H_5PW_{12}O_{42}^{-2}$ would then decrease upon protonation by the added acid and the solubility would increase. If one neglects the activity effect, then with the aid of Equations 15, 16, and 17 and the knowledge that $n = 2$,

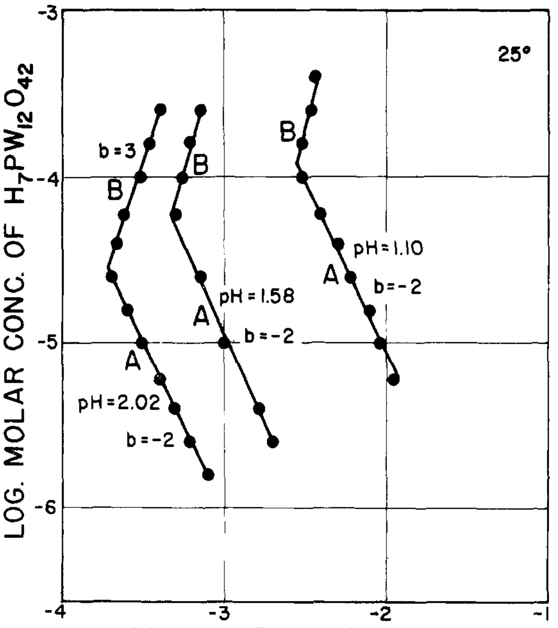

Figure 2. General solubility curves for mercurous salt of 12-tungstophosporic acid at several pH values

$$K_{sp} = K_1K_2\frac{[K_{sp}]}{[H^+]^2\,(1 + K_1/[H^+] + K_1K_2/[H^-]^2 + \ldots)} \qquad (18)$$

On the basis of earlier results (*9*), it is reasonable to assume that the concentration of triply and higher charged species is relatively small at the low pH's for which present data have been obtained. Accordingly, one may neglect all terms higher than the third in Equation 18, and since the authors have obtained values of $[K_{sp}]$ at three different pH's Equation 18 can be solved for K_{sp}, K_1, and K_2. However, no meaningful values for these quantities were obtained, presumably because activity effects are actually appreciable at these low pH's (pH < 2).

Finally, the significance of range *B* (Figure 2) is to be discussed. The abrupt change in slope here with excess of heteropoly acid indicates probable formation of polynuclear complex ions. Anionic ion exchangers were utilized to show the existence of such complexes. An Amberlite IRA 400 ion exchange resin was saturated with free 12-tungstophosphoric acid and then a solution corresponding to concentration range *B* was exchanged in the column. The effluent was treated with chloride for the presence of free Hg^- ions, but they could not be detected. On the other hand, the influent solution gave a precipitate with chloride. Apparently mercury is tied up in a negative complex ion which was exchanged in the column. The complex could be broken down by chloride which releases Hg_2Cl_2 and accounts for the positive test with the influent.

Graphical analysis of the general solubility curve in range *B* obtained by using the same principles as described before and based for this specific case on the equilibrium

$$Hg_2HPW_{12}O_{40}(s) + n\,H_5PW_{12}O_{42}^{-2} + 2H_2O \rightleftarrows Hg(H_5PW_{12}O_{42})_{n+1}^{-2n} \qquad (19)$$

results in the relationship

$$b = 1/n \qquad (20)$$

Since slope *b* is equal to 3 in range *B*, the complex appears to be $Hg_6(H_5PW_{12}O_{42})_4^{-2}$. Independent methods will be necessary to confirm the existence and structure of such polynuclear ionic species.

Mercurous 9-Tungstophosphate. General solubility curves for mercurous 9-tungstophosphate are presented in Figure 3. Again, the two ranges are denoted by *A* and *B*. The slope of the lines in range *A* at pH = 2.61 and 2.32 is −6, which indicates that the composition of the solid phase is the normal salt, $Hg_6P_2W_{18}O_{62}$. At lower pH's, the slope decreases, indicating formation of acid salts. This is apparently due to the shift in the ionization equilibrium of the 9-tungstophosphoric acid with pH. Since the shift of slope is continuous, fractional slopes being obtained, it would appear that at these lower pH's the solid phase is a mixture of at least two species. For pH = 2.61 and 2.32 where the composition of the solid phase is definite, an apparent solubility product was calculated, defined analogously to Equation 17. The values are 4×10^{-28} at pH = 2.61 and 5×10^{-27} at pH = 2.32. As for the 12-acid, this change is probably due to the combined influence of the added acid upon ionization equilibria and upon the activities of the various species. As pH increases above 2.61, the tendency for formation of complex ions is much stronger and this considerably narrows range *A*. At pH = 3.3 to 3.7 the entire investigated range of the solubility curve corresponds to range *B* for the other curves.

The effects in range *B* are very difficult to interpret at low pH's because of rather high concentrations of precipitating components and the composition of the solid phase is not known.

However, for pH = 2.32 where the composition of the solid phase is known, a graphical analysis similar to that described for mercurous 12-tungstophosphate was performed. The probable constitution of the complex ions in excess of 9-tungstophosphate ion can be obtained from the equilibrium:

$$Hg_6P_2W_{18}O_{62}(s) + n\,P_2W_{18}O_{62}^{-6} \rightleftarrows Hg_6(P_2W_{18}O_{62})_{n+1}^{-6n} \qquad (21)$$

The slope in range *B* at pH = 2.61 is precisely 1, which gives *n* = 1. Thus, the complex appears to be a dimer, $Hg_6(P_2W_{18}O_{62})_2^{-6}$. The similarity between this complex and the one obtained with the 12-tungstophosphate, $Hg_6(H_5PW_{12}O_{42})_4^{-2}$ is rather striking, both involving six Hg^+ ions and four central phosphorus atoms.

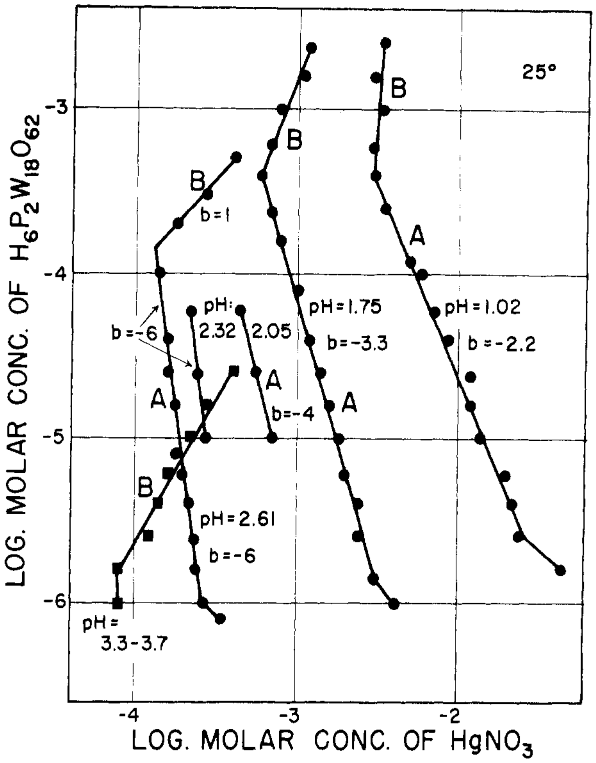

Figure 3. General solubility curves for mercurous salt of 9-tungstophosphoric acid at several pH values

LITERATURE CITED

(1) Barbieri, A.G., *Atti. accad. Lincei* [5] **23**, 805 (1914).

(2) Bradley, A.J., Illingworth, J.W., *Proc. Roy. Soc. (London)* **A157**, 113 (1936).

(3) Chow, Adam, Ms. thesis, Clarkson College of Technology, Potsdam, N.Y., 1956.

(4) Hückel, Walter, "Structural Chemistry of Inorganic Compounds," Elsevier, New York, 1950.

(5) Keggin, J.F., *Proc. Roy. Soc. (London)* **A144**, 75 (1934).

(6) Kratohvil, J.P., Tezak, Bozo, Vouk, V.B., *Arhiv kem.* **26**, 191 (1954).

(7) Matijevic, Egon, *Chimia (Switz.)* **9**, 287 (1955).

(8) Matijevic, Egon, Kerker, Milton, *J. Am. Chem. Soc.* **81**, 1307 (1959).

(9) *Ibid.*, p. 5560.

(10) Mellor, J.W., "Comprehensive Treatise on Inorganic and Theoretical Chemistry," Vol. **XI**, pp. 867, 874, Longmans, Green, New York, 1931.

(11) Pauling, Linus, *J. Am. Chem Soc.* **51**, 2868 (1929).

(12) Rakovskii, A.V., Nikitina, E.A., *J. Gen. Chem. (U.S.S.R.)* **6**, 50 (1936).

(13) Schulz, Karlo, Tezak, Bozo, *Arhiv kem.* **23**, 200 (1951).

(14) Signer, R., Gross, H., *Helv. Chim. Acta* **17**, 1076 (1934).

(15) Treadwell, E.P., Hall, W.T., "Analytical Chemistry," Vol. **II**, 9th English ed., Wiley, New York, 1948.

(16) Vouk, V.B., Kratohvil, J.P., Tezak, Bozo, *Arhiv kem.* **25**, 219 (1953).

(17) Wells, A.F., "Structural Inorganic Chemistry," Oxford Univ. Press, London, 1950.

RECEIVED for review April 29, 1960. Accepted November 15, 1960. Work supported by U.S. Atomic Energy Commission under Contract No. At (30-1) 1801.